AD_____
(Leave blank)

Award Number: W81XWH-08-1-0323

TITLE: Quantitative In Vivo Imaging of Breast Tumor Extracellular Matrix

PRINCIPAL INVESTIGATOR: Xiaoxing Han

CONTRACTING ORGANIZATION:
University of Rochester
Rochester, NY 14642

REPORT DATE: May 2010

TYPE OF REPORT: Annual Summary

PREPARED FOR: U.S. Army Medical Research and Materiel Command
Fort Detrick, Maryland 21702-5012

DISTRIBUTION STATEMENT: (Check one)

✓ Approved for public release; distribution unlimited

REPORT DOCUMENTATION PAGE

Form Approved
OMB No. 0704-0188

1. REPORT DATE *(DD-MM-YYYY)*	2. REPORT TYPE	3. DATES COVERED *(From - To)*
31-MAY-2010	Annual Summary	1 MAY 2009-30 APR 2010

4. TITLE AND SUBTITLE

Quantitative In Vivo Imaging of Breast Tumor Extracellular Matrix

5a. CONTRACT NUMBER

5b. GRANT NUMBER
W81XWH-08-1-0323

5c. PROGRAM ELEMENT NUMBER

6. AUTHOR(S)

Xiaoxing Han

Email: hanxxcn@yahoo.com

5d. PROJECT NUMBER

5e. TASK NUMBER

5f. WORK UNIT NUMBER

7. PERFORMING ORGANIZATION NAME(S) AND ADDRESS(ES)

University of Rochester
Department of Biomedical Engineering
601 Elmwood Avenue Box 639
Rochester, NY 14642

8. PERFORMING ORGANIZATION REPORT NUMBER

9. SPONSORING / MONITORING AGENCY NAME(S) AND ADDRESS(ES)
U.S. Army Medical Research and Materiel Command
Fort Detrick, Maryland 21702-5012

10. SPONSOR/MONITOR'S ACRONYM(S)

11. SPONSOR/MONITOR'S REPORT NUMBER(S)

12. DISTRIBUTION / AVAILABILITY STATEMENT
Distribution Unlimited

13. SUPPLEMENTARY NOTES

14. ABSTRACT

SHG intensity combined with the F/B ratio provides unique measures of the local density of ordered collagen, as well as the characteristic length scale of this ordering. In order to fully implement F/B ratio measurements to understand the dynamic ordering of collagen in living tumors, we must be able to measure this property *in vivo*, in intact tissue, which stops us from using a forwards detector. In this annual report, we described ongoing work developing optical methods to quantify the breast tumor collagen SHG F/B scattering ratio in intact tumors *in vivo*, i.e. without a forwards detector. In future studies this information will be used to determine how manipulation of gene expression by tumor associated macrophages affects collagen ordering, and to determine if SHG measurement of collagen ordering provides a clinically useful measure of metastatic ability.

15. SUBJECT TERMS
Breast Tumor, Collagen, SHG, F/B ratio, In vivo microscopy

16. SECURITY CLASSIFICATION OF:			17. LIMITATION OF ABSTRACT	18. NUMBER OF PAGES	19a. NAME OF RESPONSIBLE PERSON
a. REPORT	b. ABSTRACT	c. THIS PAGE			USAMRMC
U	U	U	UU	30	19b. TELEPHONE NUMBER *(include area code)*

Standard Form 298 (Rev. 8-98)
Prescribed by ANSI Std. Z39.18

Table of Contents

Page

Introduction

Recently, second harmonic generation (SHG) has proven to be a useful window into the amount and organization of fibrillar collagen in biological tissues due to its relative specificity and the fact that it is an intrinsic signal [1–6]. SHG is a coherent phenomenon, which implies that SHG is sensitive not only to the amplitude of the illumination field but also to its phase. In addition to a spatial resolution that is equal to other imaging techniques (such as two photon excited fluorescence), SHG microscopy can provide information about the sample's molecular structure. For example, the ratio of the forward-propagating to backward propagating SHG signal (the "F/B ratio") can help us to understand the axial extent of ordering in collagen fibers [1–5].

The internal ordering of collagen fibers within a tumor is a significant factor in the process of tumor metastasis. In breast tumor experiments in mice, tumor cells prefer to move along fibers that are visible by second harmonic generation [3]. Furthermore, tumor cells that are moving along SHG-producing collagen fibers move significantly faster than those cells that are not [4]. Lastly, treatment of tumors with the hormone relaxin, known to alter metastatic ability, has been shown to alter the collagen ordering, detectable by SHG but not by conventional staining [2]. We therefore believe that the assembly of collagen into ordered fibers, visible with SHG, is an important step in tumor metastasis. And by measuring SHG F/B ratio of tumor collagen, we would be able to get information about internal ordering of tumor collagen fibers and even predict metastasis.

Previously, in vitro measurements of SHG F/B ratios have been used to study collagen fiber ordering in various tissue samples such as rat tail, ovarian cancer biopsies, mouse models of breast cancer, and dermis from mouse models of Osteogenesis Imperfecta (OIM) [1–5,7]. The F/B ratio revealed the length scale of ordering in the fibers. In these measurements a second objective lens was needed to collect forward propagating SHG signal. Hence, the tissue sample had to be dissected from the animal and sectioned to 100um slices to allow signal to reach the second detection lens. For clinical application, such as in endoscopy, it is impossible to put an objective and a PMT detector underneath the tissue sample to collect the forward propagating SHG. The excision and sectioning required to use a second detector for forward propagating SHG also prevents dynamic measurements of collagen ordering over time. Therefore, it becomes highly desirable to develop a new optical system to measure collagen SHG F/B ratio in vivo, using only epi-detection and on intact thick tissue samples.

Body

We are now concluding the second year of this grant, here in the Department of Biomedical Engineering at the University of Rochester Medical Center. The work we have done for both the research and training plans are listed below:

Research Plan

Hypothesis1. The ratio of forward- to backward-scattered SHG signal can be accurately imaged and quantified in breast tumor models *in vivo* and in excised biopsy sections

Specific Aim 1a: Determine if the method of direct collection of forward-scattered SHG signal is feasible.

This specific aim had been accomplished and discussed in detail in my past publication[4], and my first year annual report.

Specific Aim 1b: Determine if the collection of forward-scattered SHG signal via a confocal aperture mirror is feasible.

This specific aim was accomplished and published in our recent paper [12] from which much of the text of this report has been taken. For this specific aim we modified our original plan a little bit according to our new data. Instead of the original confocal aperture mirror plan described in our proposal, we measured collagen fiber SHG F/B ratio in vivo with five pinholes of different pinhole sizes. These pinholes are already built in the variable pinhole turret available in most commercial two photon microscopes. With this variable pinhole method, SHG F/B ratio can be measured in vivo on any commercial two photon microscopes with minimal purchase of new equipment.

Also considering the availability of the sample, in the experiment, we used rat tail in stead of breast tumor tissue as sample, since it usually takes longer time for breast tumors to grow.

1 Optical setup

The optical setup we are using to determine the SHG F/B ratio *in vivo* using only epidetection is shown in Figure 1 below. SHG signal was generated by a Spectra Physics MaiTai Ti:Sapphire laser providing 100fs pulses at 80 MHz and 810 nm. The excitation beam was directed into an Olympus Fluoview F300 scanhead connected to an Olympus BX61WI upright microscope. The focusing objective is an Olympus UMPLFL20XW water immersion lenses (20×, 0.5 N.A.). This objective was used to focus the excitation beam on the sample and at the same time collect the direct backward-propagating SHG as well as the forward-propagating SHG signal that was subsequently backscattered within the tissue. The SHG signal was collected by the objective, converged by the tube lens, and collimated by the pupil lens. The collimated SHG beam was then de-scanned and focused again on the pinhole plane by the collector lens. All of these lenses are intrinsic to the BX61WI microscope or the

Fluoview F300 scanhead. The focal lengths of the pupil lens and the collector lens are 54mm and 185mm respectively, and size of the pinholes on the F300 variable pinhole turret are 60um, 100um, 150um, 200um and 7000um. The SHG beam was separated from the excitation beam by a dichroic mirror (Chroma 670 DCSX) inserted into the F300 scanhead, as well as a band pass filter centered at 405 nm (Chroma HQ405/30m-2P) placed after the pinhole, and detected by the FV300's intrinsic photomultiplier tubes. The only significant equipment modifications are insertion of the aforementioned dichroic mirror and filter in the appropriate location in the scanhead, and the punching out of one of the pinholes in the pinhole turret to produce one extremely large pinhole setting (see below).

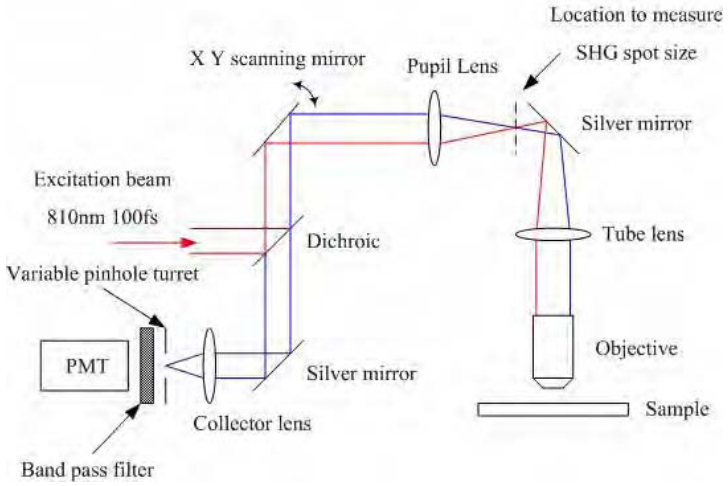

Fig. 1. Experimental setup for *in vivo* measurement of collagen SHG F/B ratio

2 SHG Back Scattering and Monte Carlo Simulation

Using the apparatus described above, we generate an SHG image using confocal detection of the resultant SHG. While much of the forward-propagating SHG signal will travel into the tissue sample and be lost to our objective lens, a fraction of this signal undergoes multiple scattering events and passes back through the object plane, traveling towards the objective lens. As shown in Figure 2, this signal will pass through the object plane at multiple locations. Conversely, at shallow imaging depths the backwards-propagating SHG signal will emanate from the image plane only from the two-photon focal volume with minimal subsequent scatter. When the object plane is imaged onto the confocal pinhole, the spatial distribution of SHG signal on the confocal plane will consist of a sharp central peak due to the backward propagating SHG plus a diffuse signal due to the forwards propagating and subsequently backscattered SHG. As discussed below, our new method consists of repeatedly imaging the sample through a series of different sized pinholes, whereby the shape of this total SHG distribution can be measured and, with suitable calibration, the underlying F/B ratio can be determined.

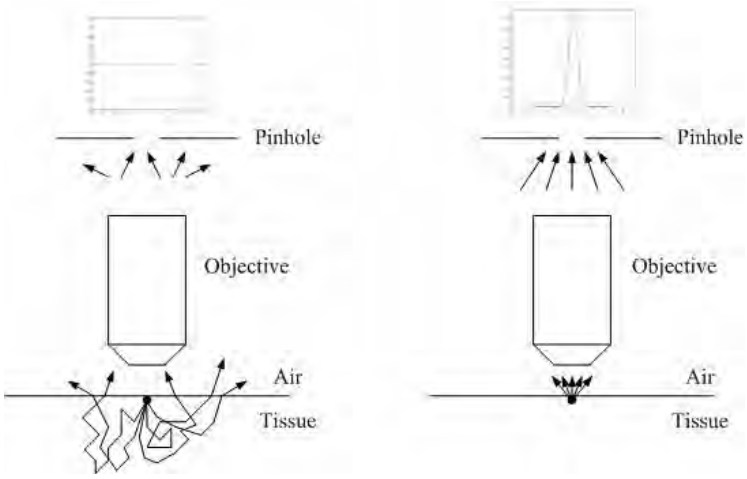

Fig. 2. Back scattering of forward-propagating SHG and propagation of direct backward propagating SHG

In order to implement this method we must first understand the spatial distribution, in the object plane, of forward propagated light that subsequently backscatters and reaches that plane. 405 nm SHG signal is easily scattered while propagating in the tissue sample. In Legare et al 2007 [8], it was determined that ~21% of the forward-propagating SHG signal was subsequently backscattered and reached the tissue surface, and that the epi-detected image from a 5mm thick Achilles tendon tissue block was actually a combination of the direct backward propagating SHG signal and the forward propagating SHG signal that was subsequently backscattered. In fact for collagen fibers in some tissue samples, such as in mouse breast tumor models, the SHG F/B ratio is very high (~30) [4], and most SHG signal propagates in the forward direction. In these cases epi-detected SHG microscopy is greatly enhanced due to the subsequent backscattering of the forward propagating SHG.

The propagation of light in turbid media can be well modeled by Monte Carlo simulation of the paths that photons make as they travel through tissue, which are chosen by statistically sampling the probability distributions for step size and angular deflection per scattering event. Using a Monte Carlo code based closely upon that of Wang et al [9] (see Appendix), we sent 405nm SHG photons into an infinitely deep scattering tissue in the forward direction. The SHG photons were emitted from a point source and we ignored the direct backward propagating SHG photons. We experimentally measured the angular distribution of the forward propagating SHG emission by imaging the back focal plane of an objective lens which was collecting the forward propagating SHG from a 10 um thin section of tumor tissue, and found that the forward SHG from collagen fibers is emitted in a rather tight beam confined to +/-15 degrees around the laser axis (data not shown). Hence we used the same initial angular distribution (+/-15 degrees around the axis normal to the tissue-air surface) in the Monte Carlo simulation. The scattering particles are modeled as 10um diameter cells, the refractive indexes inside and outside of the cells are 1.38 and 1.42 respectively, and the scattering and absorption coefficients we used in the simulation are μ_a=0.7 cm^{-1} and μ_s=150 cm^{-1} [10]. The probability distribution of scattering angles after every scattering event were calculated according to Mie theory with the cell size

and the refractive index inside and outside of the cells, with a 99% chance the scattering angle will fall between +/-6 degrees. We then counted the number of photons which escape from the air-tissue surface in the backward direction and plotted out the steady state distribution of the backscattered photons over the radial distance from the emission point.

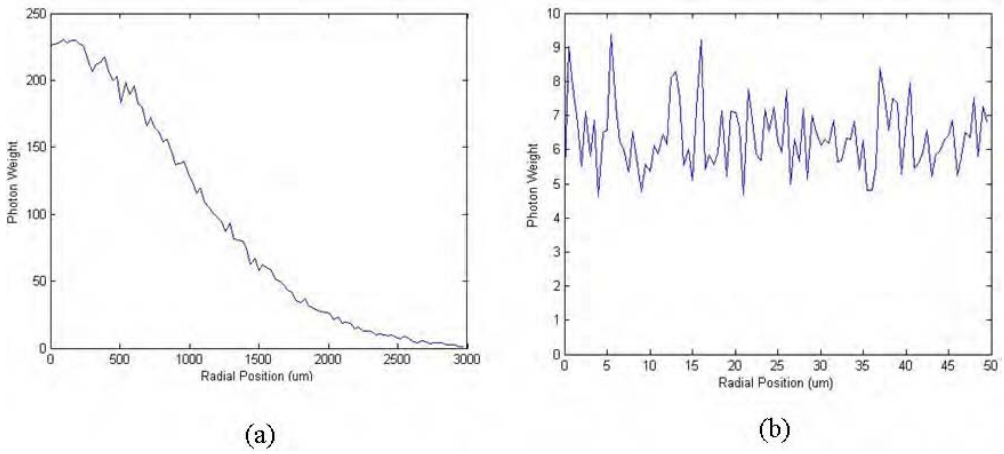

Fig. 3. Monte Carlo simulation of forward propagating and subsequently backscattered SHG photons which reach the object plane.(a) Steady state radial distribution of the backscattered SHG photons over a large range of radial position (3mm) (b) The same distribution over a short radial range (50um)

The simulation results are shown in Figure 3. Figure 3a shows the steady state distribution of the forward propagating and subsequently backscattered SHG photons which reach the object plane, over a large range of radial positions i.e. from the center to 3mm away from the emission point. Figure 3b shows the same distribution over a short range i.e. from the center to only 50um away from the emission point, which is the length scale of our largest pinhole setting (where the pinhole-bearing foil has been punched out). We can see from Figure 3a that over a large length scale the forward propagating and subsequently back-scattered SHG photon intensity decays exponentially with the distance from emission point, which agrees with previous literature [11]. But from Figure 3b we can see over a very short range of 50 um, the range covered by our pinhole settings and where the diffusion approximation does not hold [11], the intensity of forward propagating and subsequently back scattered SHG photons is constant and does not depend on distance from the focal volume.

3 Fitting model

To measure collagen fiber SHG F/B ratio in vivo with only the epi-detection objective, we will generate a series of collagen fiber SHG images, in the backward channel, through a series of confocal pinholes of different sizes which correspond to a diameter in the object plane ranging from 0.874 um to 102 um (see 3.1 below). As discussed above, the SHG signal we collect after the pinhole is a mixture of both the direct backward propagating SHG and the forward propagating and subsequently backscattered SHG. To analyze our experimental data we model the image in the pinhole plane of the direct backward propagating SHG signal plane as a Gaussian spot

[12], while the forward propagating SHG that subsequently backscatters is modeled as a uniform distribution over these length scales (based upon the results of our Monte Carlo simulation, as described above). So the total SHG signal intensity distribution on the object plane can be expressed as:

$$I_{SHG}(r) = B\exp[-2(\frac{r}{\omega})^2] + FC \qquad (1)$$

Where ω is the e-2 Gaussian spot size of the direct backward propagating SHG, F and B are absolute intensities of forward and backward propagating SHG signals, the parameter C relates the initial forward propagating signal intensity to the average intensity of the uniform distribution of SHG light that reaches the object plane, and is a function of scattering and absorption properties of the underlying tissue. Alternatively, this expression can be written in another way,

$$I_{SHG}(r) = B[\exp[-2(\frac{r}{\omega})^2] + \frac{F}{B}C] \qquad (2)$$

where F/B represents the collagen fiber SHG F/B ratio.

When we generate collagen fiber SHG images through a series of confocal pinholes of different sizes, each pixel on that image represents an integration of the total SHG signal over the pinhole area

$$I_{pixel} \propto \int_0^{2\pi} d\theta \int_0^{R} \left\{ \exp[-2(\frac{r}{\omega})^2] + \left(\frac{F}{B}\right)C \right\} r dr \qquad (3)$$

where R is the size of the pinhole with respect to Gaussian spot size of the direct backward propagating SHG, i.e. $R=r_{pinhole}/\omega$. If the pixel intensities at various pinhole sizes are normalized to the maximum pixel intensity at the largest pinhole size, the relative pixel intensity is a function of relative pinhole size R:

$$I_{rel}(R) = \frac{\int_0^{2\pi} d\theta \int_0^{R} \left\{ \exp[-2(\frac{r}{\omega})^2] + \left(\frac{F}{B}\right)C \right\} r dr}{\int_0^{2\pi} d\theta \int_0^{R_{max}} \left\{ \exp[-2(\frac{r}{\omega})^2] + \left(\frac{F}{B}\right)C \right\} r dr} \qquad (4)$$

where R_{max} is the largest pinhole size in our system. With this expression we can plot the relative pixel intensity versus pinhole size and fit the data to produce (F/B)C. In order to determine F/B we must then eliminate C, the fraction of signal which originally propagates in the forward direction but is eventually backscattered by the tissue and reaches the pinhole plane. This can be done by introducing into the sample a reference of known F/B ratio, whose C value is the same. In these experiments we used blue fluorescent polystyrene beads (peak λem=424nm) sprinkled onto the sample surface. The quantity (F/B)C is then determined for both the calibration beads in the image, as well as the fibers of interest. Next, the correction factor that is required to convert the measured values of bead (F/B)C to the known value of F/B is determined, and the previously unknown value of fiber F/B is determined from the measured

(F/B)C using the same correction factor:

$$\frac{measured\ collagen\ SHG\ F\ /\ B\ Ratio}{measured\ beads\ TPEF\ F\ /\ B\ Ratio} = \frac{real\ collagen\ SHG\ F\ /\ B\ Ratio}{real\ beads\ TPEF\ F\ /\ B\ Ratio} \quad (5)$$

To illustrate the fitting function given by equation 4 in the case of the typical backscattering fraction C=0.001 and Rmax=28 we can plot out the relative pixel intensity v.s. pinhole size curves at various collagen fiber SHG F/B ratios:

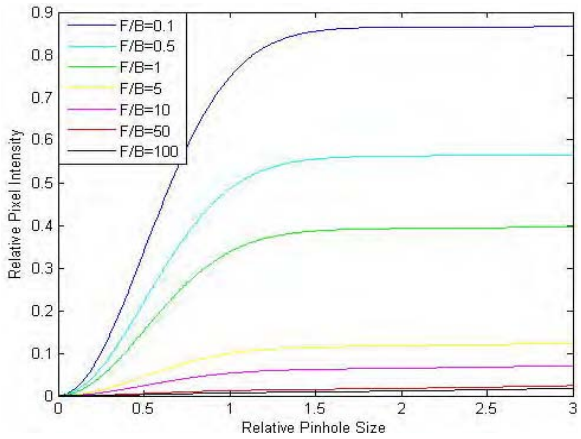

Fig 4. Relative SHG intensity vs. relative pinhole size curves at different collagen SHG F/B ratios, based upon equation 4. The relative SHG intensities equal 1 at a pinhole size of $r=R_{max}=28$.

From this plot one can see the sharp curvature due to the Gaussian distribution of direct back-propagating SHG (most evident in the steep early rise of the curves with small values of F/B) and the slow and steady rise due to forward-propagating light that is subsequently backscattered and produces a diffuse signal which does not vary with r (most evident in the slow rise of the curves with large values of F/B). This reveals the utility in punching out one of the metal foils containing a pinhole from the pinhole turret of the scanner, as this produces one pinhole of extremely large size (R=28 in the case of the Fluoview 300) whose radius is far from the initial sharp curvature due to the Gaussian distribution of direct back-propagating SHG, allowing the collection of a great deal of the diffuse forward-propagated signal.

4 Measurement of SHG intensity varied with pinhole size

To evaluate our new method we chose the rat tail tendon, a sample whose SHG properties have been well studied [1]. A whole rat tail was removed from a previously sacrificed animal (removal from the animal is not necessary for the technique but is convenient for handling the sample). To generate a clear SHG image of the tendon in particular (to match the sample previously studied in the literature) we peeled a thin layer of outer skin off the rat tail at the location of interest and exposed the tendon beneath it. We then put the rat tail on a glass slide, with the exposed collagen fiber facing up and we put another coverslip on top of the collagen fibers to ensure a stable sample. The rat tail and coverslip were then fixed on the glass slide with plastic tape

and the collagen fibers were imaged though the coverslip. Note that, unlike previous methods which measure F/B with a second detector for the forward-propagating SHG, the tendons remained within the ~1cm diameter tail.

We prepared whole rat tail samples from 5 separate animals. On each rat tail we chose 5 image fields. And for each image field we took 5 back detected SHG images with the pinhole size varied from 60um 100um 150um 200um to 7000um, plus one image with no sample in order to quantify the background noise. One of these image sets is shown below.

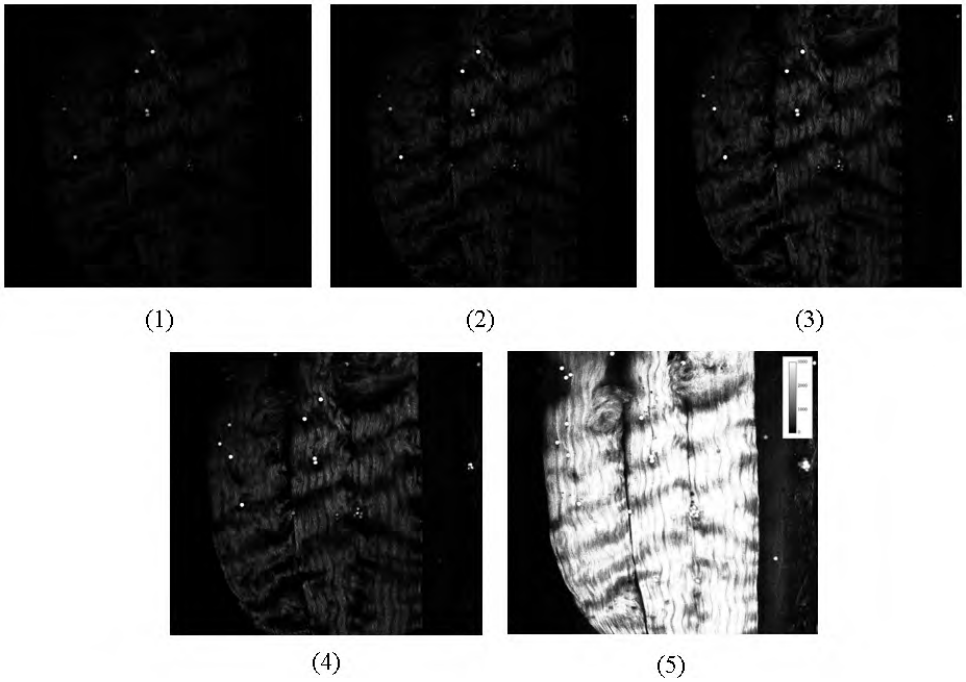

Fig. 7 *In vivo* SHG images of rat tail collagen fibers in an intact rat tail. Images 1-5 are SHG images of the same ROI when the size of the pinhole varied from 60um, 100um, 150um, 200um, to 7000um, respectively. The bright spots are blue fluorescent polystyrene beads for calibration. Images are 600 um across.

5 Curve fitting and prediction of collagen SHG F/B ratio

In each set of images, we picked 5 small regions of interest (ROIs) around collagen fibers and 3 regions of interest around the calibration beads. ROIs were drawn around fibers that extended over at least ~100 um in the image plane, to ensure that fibers were close to perpendicular to the optical axis. A length 100 um in an optical section of ~12 um thickness (e-2 z diameter of the PSF) corresponds to a maximum angle in the object plane of ~7 degrees. Signal intensities in these collagen and beads ROIs were measured with ImageJ, background was subtracted, and signal intensities were normalized so that the maximum intensity measured with the largest pinhole was set to 1. The average relative SHG intensity of all 25 collagen ROIs (5 ROIs in each of 5 image stacks) and average relative TPEF intensity of all 15 beads ROIs in one rat tail vs. relative pinhole size plot is shown below. Note the separation between the

collagen fiber curve and the bead curve due to the different F/B ratios of rat tail collagen and fluorescent calibration beads.

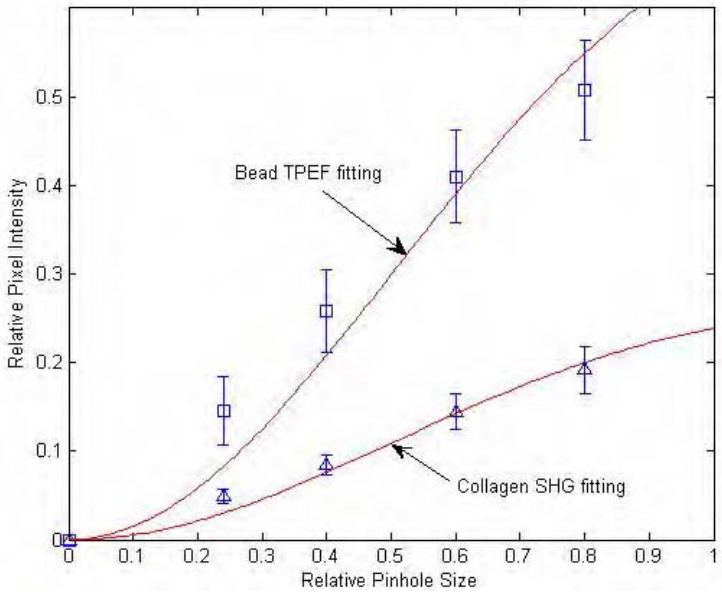

Fig. 8 Epidetected total collagen SHG intensity (blue triangles), or total bead TPEF intensity (blue squares) vs. pinhole size, fit to the model given by equation 4 (red lines). The horizontal axis is pinhole size in units of backward propagating SHG spot size on the pinhole plane i.e. fraction of ω. The vertical axis is normalized SHG intensity. Note that the fitting curves identically equal 1 when the pinhole size reaches R=28, whose data point is not shown, and that the intensity information for R=28 provides the normalization value and hence is included in the overall fit.

As described above, for one rat tail we measured relative intensity in 25 collagen ROIs and 15 bead ROIs. For each ROI 5 relative intensities were measured with size of the pinhole varying from the smallest to the largest. Average relative SHG intensity of all 25 collagen ROIs and average relative TPEF intensity of all 15 bead ROIs, as shown in figure 8, were considered a set of data for one rat tail. We then fit this set of real measured data to the model given in equation (4) and calculated the rat tail collagen fiber SHG F/B ratio in one animal by eliminating C using equation (5). This data collection/averaging/curve fitting/calculation process was repeated 5 times to calculate rat tail collagen fiber SHG F/B ratio in 5 animals. The results are listed in the table below.

	Animal I	Animal II	Animal III	Animal IV	Animal V	Average
F/B ratio	2.10±0.19	1.81±0.30	2.50±0.34	1.34±0.13	2.26±0.23	2.00±0.45

Table 1. Results of *in vivo* measured rat tail collagen SHG F/B ratio. For each animal, means ± 95% confidence intervals are presented, with the data from 25 ROIs being pooled to produce a single curve fit for each animal. The average value for the 5 animals is then presented ± the standard deviation.

To verify the validity of our method using thick samples and only epi-detection, we also directly measured rat tail collagen SHG F/B ratio with both forward and backward detectors and with the sample sectioned in ~10um thin slices, as previously described [4]. In summary, the SHG image captured in the forward detector was

divided by the SHG image captured in the backward detector. We then averaged SHG F/B ratio over all pixels within collagen fibers and ignored all pixels outside the collagen fibers. The scattering of the tissue, though very low in this case, was corrected for by measuring the F/B ratio of the TPEF signals from 10um diameter calibration fluorescent beads.

The measurement results from 5 animals, using forward and backwards detectors, are listed in the table below:

	Animal VI	Animal VII	Animal VIII	Animal IX	Animal X	Average
F/B ratio	1.43±0.80	1.22±0.27	2.29±0.49	1.75±0.50	2.11±0.86	1.76±0.45

Table 2. Results of *in vitro* measured rat tail collagen SHG F/B ratio For each animal, means ± standard deviations are presented from 5 F/B measurements. The average value for the 5 animals is then presented ± the standard deviation.

The overall average F/B ratio from 5 animals is 1.76+/-0.45. This result was not statistically significantly different from our measurement using only the epi-detection objective lens and the model given by equation (4) (Student's t-test p=0.42) demonstrating that the results from the two methods are in good agreement. To evaluate the new method at a higher NA we also measured the F/B ratio using a 0.8 NA lens, producing a value for F/B (1.37+/-0.28) which is again not statistically significantly different from the direct measurement using forward and backwards detectors (p=0.17 N=5).

Hypothesis 2. The ratio of forward- to backward-scattered SHG signal accurately quantifies collagen turnover in breast tumors models *in vivo*.

Hypothesis 3. The F/B ratio predicts tumor metastasis.

We anticipate further developing our pinhole mirror technique next year, and in parallel pursuing Hypotheses 2 and 3.

Training Plan

Task 1. Continue formal education in oncology

I have taken the Harvard Medical School Continuing Education Course "Critical Issues in Tumor Microcirculation, Angiogenesis, and Metastasis" in the summer of 2009, and we have planned to take the PTH 507 Cancer Biology and the Radiation Biology course next semester.

Task 2. Continue formal education in optics.

I have completed the course OPT 568 Waveguide Optoelectronic Devices,

Task 3. Continue informal education in oncology.

I have learned a lot about tumor biology by listening to the presentations in our group meeting every week and attending the local journal club and lectures.

Task 4. Continue informal education in optics.

I have attended OSA BIOMED and Frontier in Optics (FIO) conferences and contributed poster presentations in those meetings. I regularly attended the local journal club and lectures at the Institute of Optics. I also attended our group meeting every week.

Task 5. Laboratory training.

I have learned to prepare the dorsal skin fold chamber and grow passage and implant breast tumor cells. I am familiar with biological techniques such as northern blotting and histological stains. I am experienced in optical alignment and all other optics experiments. And I am capable to do project design, experiment design, trouble shooting and data analysis.

Key Research Accomplishments in the Past Year

1) We have built up a confocal SHG system to measure the tumor collagen SHG F/B ratio only in the backward direction.
2) We have written a Monte Carlo simulation Matlab code to simulate forward propagating SHG light propagation in tumor tissue.
3) With the Monte Carlo simulation result, we studied the radial intensity distribution of TPEF(fluorescent beads) or SHG(collagen fibers) signal on the confocal pinhole plane and set up a theoretical model for the back detected total TPEF or SHG signal vs. pinhole size data.
4) We experimentally measured back detected total TPEF or SHG signal vs. pinhole size data.
5) We fitted the experimental data to the theoretical model and successfully measured collagen SHG F/B ratio. We also compared our results from this new *in vivo* method to the results we get from traditional direct measurement, and found out that results from these two different methods are not significantly different.

Reportable outcomes

During the past year, a new Optics Express paper was published:
Xiaoxing Han and Edward Brown, "Measurement of the ratio of forward-propagating to back-propagating second harmonic signal using a single objective," Opt. Express **18**(10): 10538-10550

We are currently applying for a new US patent:
Edward Brown and Xiaoxing Han “Epidetection Method and Apparatus for Measuring the Ratio of Forward- Propagating to Back-Propagating Second Harmonic Signal”

We also submitted an abstract to the OSA Frontiers in Optics meeting that will be held in Oct, 2010 in Rochester, NY:
Xiaoxing Han and Edward Brown, “Epi-detected ratio of forward-propagating to back-propagating second harmonic signal” submitted to Frontiers in Optics (FiO) 2010

Conclusion

In the past year, we have successfully developed a new method to study collagen SHG F/B *in vivo*. We have also proved its validity by measuring collagen SHG F/B ratio in various samples with this new method and comparing the results we got from this new method to those we got from traditional direct measurement. Our next step would be to study the relationship between collagen SHG F/B with collagen turn over and breast tumor metastasis with this new method *in vivo*, as listed in hypothesis 2 and hypothesis 3. These facts suggest that we are making significant progress, progress

that has been enabled by the generous support of the BCRP Predoc Traineeship Award.

References

[1] R. M. Williams, W. R. Zipfel, and W. W. Webb, “Interpreting second-harmonic generation images of collagen I fibrils,” Biophys. J. 88(2), 1377–1386 (2005).

[2] R. Lacomb, O. Nadiarnykh, and P. J. Campagnola, “Quantitative second harmonic generation imaging of the diseased state osteogenesis imperfecta: experiment and simulation,” Biophys. J. 94(11), 4504–4514 (2008).

[3] O. Nadiarnykh, R. B. Lacomb, P. J. Campagnola, and W. A. Mohler, “Coherent and incoherent SHG in fibrillar cellulose matrices,” Opt. Express 15(6), 3348–3360 (2007).

[4] X. Han, R. M. Burke, M. L. Zettel, P. Tang, and E. B. Brown, “Second harmonic properties of tumor collagen:determining the structural relationship between reactive stroma and healthy stroma,” Opt. Express 16(3), 1846–1859 (2008).

[5] A. C. Kwan, D. A. Dombeck, and W. W. Webb, “Polarized microtubule arrays in apical dendrites and axons,”Proc. Natl. Acad. Sci. U.S.A. 105(32), 11370–11375 (2008).

[6] S. V. Plotnikov, A. C. Millard, P. J. Campagnola, and W. A. Mohler, “Characterization of the myosin-based source for second-harmonic generation from muscle sarcomeres,” Biophys. J. 90(2), 693–703 (2006).

[7] O. Nadiarnykh, R. B. LaComb, M. A. Brewer, and P. J. Campagnola, “Alterations of the extracellular matrix in ovarian cancer studied by second harmonic generation imaging microscopy,” BMC Cancer 10(1), 94 (2010).

[8] F. Légaré, C. Pfeffer, and B. R. Olsen, “The role of backscattering in SHG tissue imaging,” Biophys. J. 93(4), 1312–1320 (2007).

[9] L. Wang, and S. L. Jacques, “Hybrid model of Monte Carlo simulation and diffusion theory for light reflectance by turbid media,” J. Opt. Soc. Am. A 10(8), 1746–1752 (1993).

[10] W. F. Cheong, S. A. Prahl, and A. J. Welch, “A review of the optical properties of biological tissues,” IEEE J. Quantum Electron. 26(12), 2166–2185 (1990).

[11] T. J. Farrell, M. S. Patterson, and B. Wilson, “A diffusion theory model of spatially resolved, steady-state diffuse reflectance for the noninvasive determination of tissue optical properties in vivo,” Med. Phys. 19(4), 879–888 (1992).

[12] Xiaoxing Han and Edward Brown, "Measurement of the ratio of forward-propagating to back-propagating second harmonic signal using a single objective," Opt. Express 18, 10538-10550 (2010)

Measurement of the ratio of forward-propagating to back-propagating second harmonic signal using a single objective

Xiaoxing Han[1] and Edward Brown[2,*]

[1]*Institute of Optics, University of Rochester, Goergen Hall Box 270168, Rochester, New York 14627, USA*
[2]*Department of Biomedical Engineering, University of Rochester, Goergen Hall Box 270168, Rochester, New York 14627, USA*
**Edward_Brown@urmc.rochester.edu*

Abstract: In this paper, we present a method to determine, for the first time, the ratio of forward-propagating second harmonic (SHG) signal to back-propagating SHG signal (F/B) in vivo on the surface of intact tissue samples without any biopsy or tissue sectioning, using only epidetection (i.e., via a single objective lens). This method has the additional benefit of using the confocal detection apparatus already contained within common commercially available two-photon laser-scanning microscopes, and hence can allow the measurement of the SHG F/B ratio in vivo with minimal purchase of new equipment.

OCIS codes: (170.0170) Medical Optics and Biotechnology; (180.0180) Microscopy

References and links

1. R. M. Williams, W. R. Zipfel, and W. W. Webb, "Interpreting second-harmonic generation images of collagen I fibrils," Biophys. J. **88**(2), 1377–1386 (2005).
2. R. Lacomb, O. Nadiarnykh, and P. J. Campagnola, "Quantitative second harmonic generation imaging of the diseased state osteogenesis imperfecta: experiment and simulation," Biophys. J. **94**(11), 4504–4514 (2008).
3. O. Nadiarnykh, R. B. Lacomb, P. J. Campagnola, and W. A. Mohler, "Coherent and incoherent SHG in fibrillar cellulose matrices," Opt. Express **15**(6), 3348–3360 (2007).
4. X. Han, R. M. Burke, M. L. Zettel, P. Tang, and E. B. Brown, "Second harmonic properties of tumor collagen: determining the structural relationship between reactive stroma and healthy stroma," Opt. Express **16**(3), 1846–1859 (2008).
5. A. C. Kwan, D. A. Dombeck, and W. W. Webb, "Polarized microtubule arrays in apical dendrites and axons," Proc. Natl. Acad. Sci. U.S.A. **105**(32), 11370–11375 (2008).
6. S. V. Plotnikov, A. C. Millard, P. J. Campagnola, and W. A. Mohler, "Characterization of the myosin-based source for second-harmonic generation from muscle sarcomeres," Biophys. J. **90**(2), 693–703 (2006).
7. O. Nadiarnykh, R. B. LaComb, M. A. Brewer, and P. J. Campagnola, "Alterations of the extracellular matrix in ovarian cancer studied by second harmonic generation imaging microscopy," BMC Cancer **10**(1), 94 (2010).
8. F. Légaré, C. Pfeffer, and B. R. Olsen, "The role of backscattering in SHG tissue imaging," Biophys. J. **93**(4), 1312–1320 (2007).
9. L. Wang, and S. L. Jacques, "Hybrid model of Monte Carlo simulation and diffusion theory for light reflectance by turbid media," J. Opt. Soc. Am. A **10**(8), 1746–1752 (1993).
10. W. F. Cheong, S. A. Prahl, and A. J. Welch, "A review of the optical properties of biological tissues," IEEE J. Quantum Electron. **26**(12), 2166–2185 (1990).
11. T. J. Farrell, M. S. Patterson, and B. Wilson, "A diffusion theory model of spatially resolved, steady-state diffuse reflectance for the noninvasive determination of tissue optical properties in vivo," Med. Phys. **19**(4), 879–888 (1992).
12. W. R. Zipfel, R. M. Williams, and W. W. Webb, "Nonlinear magic: multiphoton microscopy in the biosciences," Nat. Biotechnol. **21**(11), 1369–1377 (2003).

1. Introduction

Recently, second harmonic generation (SHG) has proven to be a useful window into the amount and organization of fibrillar collagen in biological tissues due to its relative specificity and the fact that it is an intrinsic signal [1–6]. SHG is a coherent phenomenon, which implies that SHG is sensitive not only to the amplitude of the illumination field but also to its phase. In addition to a spatial resolution that is equal to other imaging techniques

#124594 - $15.00 USD Received 23 Feb 2010; revised 16 Apr 2010; accepted 19 Apr 2010; published 5 May 2010

(such as two photon excited fluorescence), SHG microscopy can provide information about the sample's molecular structure. For example, the ratio of the forward-propagating to backward propagating SHG signal (the "F/B ratio") can help us to understand the axial extent of ordering in collagen fibers [1–5].

Previously, in vitro measurements of SHG F/B ratios have been used to study collagen fiber ordering in various tissue samples such as rat tail, ovarian cancer biopsies, mouse models of breast cancer, and dermis from mouse models of Osteogenesis Imperfecta (OIM) [1–5,7]. The F/B ratio revealed the length scale of ordering in the fibers and in the case of OIM and ovarian cancer, was able to discriminate pathological tissue from healthy tissue [2,7]. In these measurements a second objective lens was needed to collect forward propagating SHG signal. Hence, the tissue sample had to be dissected from the animal and sectioned to 100um slices to allow signal to reach the second detection lens. For clinical application, such as in endoscopy, it is impossible to put an objective and a PMT detector underneath the tissue sample to collect the forward propagating SHG. The excision and sectioning required to use a second detector for forward propagating SHG also prevents dynamic measurements of collagen ordering over time. Therefore, it becomes highly desirable to develop a new optical system to measure collagen SHG F/B ratio in vivo, using only epi-detection and on intact thick tissue samples.

2. Experimental methods

2.1 Optical setup

The optical setup we are using to determine the SHG F/B ratio in vivo using only epidetection is shown in Fig. 1 below. SHG signal was generated by a Spectra Physics MaiTai Ti:Sapphire laser providing 100fs pulses at 80 MHz and 810 nm. The excitation beam was directed into an Olympus Fluoview F300 scanhead connected to an Olympus BX61WI upright microscope. The focusing objective is an Olympus UMPLFL20XW water immersion lenses (20 × , 0.5 N.A.), with supporting measurements performed using an Olympus LUMPlanFL/IR (40x, 0.8 NA) water immersion lens. This objective was used to focus the excitation beam on the sample and at the same time collect the direct backward-propagating SHG as well as the forward-propagating SHG signal that was subsequently backscattered within the tissue. The SHG signal was collected by the objective, converged by the tube lens, and collimated by the pupil lens. The collimated SHG beam was then de-scanned and focused again on the pinhole plane by the collector lens. All of these lenses are intrinsic to the BX61WI microscope or the Fluoview F300 scanhead. The focal lengths of the pupil lens and the collector lens are 54mm and 185mm respectively, and size of the pinholes on the F300 variable pinhole turret are 60um, 100um, 150um, 200um and 7000um. The SHG beam was separated from the excitation beam by a dichroic mirror (Chroma 670 DCSX) inserted into the F300 scanhead, as well as a band pass filter centered at 405 nm (Chroma HQ405/30m-2P) placed after the pinhole, and detected by the FV300's intrinsic photomultiplier tubes. The only significant equipment modifications are insertion of the aforementioned dichroic mirror and filter in the appropriate location in the scanhead, and the punching out of one of the pinholes in the pinhole turret to produce one extremely large pinhole setting (see below).

#124594 - $15.00 USD Received 23 Feb 2010; revised 16 Apr 2010; accepted 19 Apr 2010; published 5 May 2010

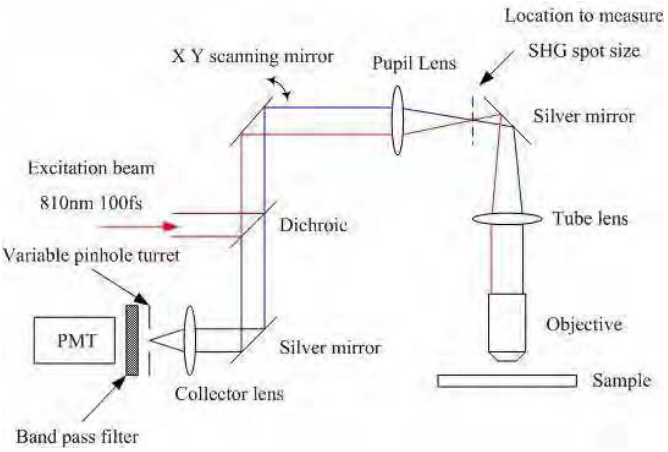

Fig. 1. Experimental setup for in vivo measurement of tumor collagen SHG F/B ratio.

2.2 SHG Back Scattering and Monte Carlo Simulation

Using the apparatus described above, we generate an SHG image using confocal detection of the resultant SHG. While much of the forward-propagating SHG signal will travel into the tissue sample and be lost to our objective lens, a fraction of this signal undergoes multiple scattering events and passes back through the object plane, traveling towards the objective lens. As shown in Fig. 2, this signal will pass through the object plane at multiple locations. Conversely, at shallow imaging depths the backwards-propagating SHG signal will emanate from the image plane only from the two-photon focal volume with minimal subsequent scatter. When the object plane is imaged onto the confocal pinhole, the spatial distribution of SHG signal on the confocal plane will consist of a sharp central peak due to the backward propagating SHG plus a diffuse signal due to the forwards propagating and subsequently backscattered SHG. As discussed below, our new method consists of repeatedly imaging the sample through a series of different sized pinholes, whereby the shape of this total SHG distribution can be measured and, with suitable calibration, the underlying F/B ratio can be determined.

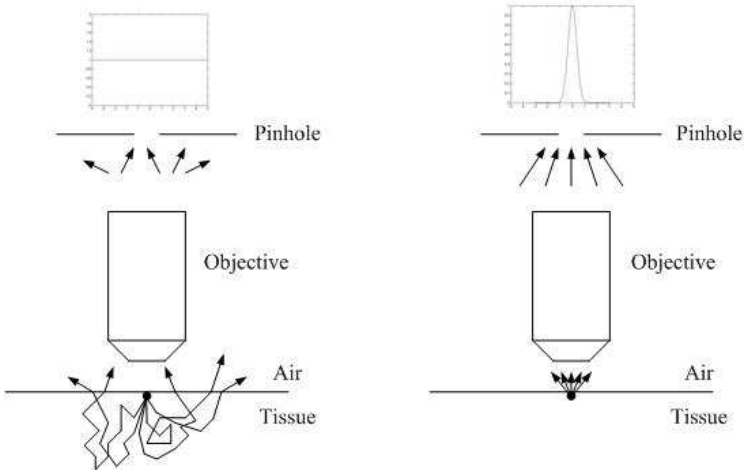

Fig. 2. Back scattering of forward-propagating SHG and propagation of direct backward propagating SHG

In order to implement this method we must first understand the spatial distribution, in the object plane, of forward propagated light that subsequently backscatters and reaches that

#124594 - $15.00 USD Received 23 Feb 2010; revised 16 Apr 2010; accepted 19 Apr 2010; published 5 May 2010

plane. 405 nm SHG signal is easily scattered while propagating in the tissue sample. In Legare et al 2007 [8], it was determined that ~21% of the forward-propagating SHG signal was subsequently backscattered and reached the tissue surface, and that the epi-detected image from a 5mm thick Achilles tendon tissue block was actually a combination of the direct backward propagating SHG signal and the forward propagating SHG signal that was subsequently backscattered. In fact for collagen fibers in some tissue samples, such as in mouse breast tumor models, the SHG F/B ratio is very high (~30) [4], and most SHG signal propagates in the forward direction. In these cases epi-detected SHG microscopy is greatly enhanced due to the subsequent backscattering of the forward propagating SHG.

The propagation of light in turbid media can be well modeled by Monte Carlo simulation of the paths that photons make as they travel through tissue, which are chosen by statistically sampling the probability distributions for step size and angular deflection per scattering event. Using a Monte Carlo code based closely upon that of Wang et al [9] (see Appendix), we sent 405nm SHG photons into an infinitely deep scattering tissue in the forward direction. The SHG photons were emitted from a point source and we ignored the direct backward propagating SHG photons. We experimentally measured the angular distribution of the forward propagating SHG emission by imaging the back focal plane of an objective lens which was collecting the forward propagating SHG from a 100 um section of tumor tissue, and found that the forward SHG from collagen fibers is emitted in a rather tight beam confined to +/−15 degrees around the laser axis (data not shown). Hence we used the same initial angular distribution (+/−15 degrees around the axis normal to the tissue-air surface) in the Monte Carlo simulation. The scattering particles are modeled as 10um diameter cells, the refractive indexes inside and outside of the cells are 1.38 and 1.42 respectively, and the scattering and absorption coefficients we used in the simulation are μa = 0.7 cm−1 and μs = 150 cm−1 [10]. The probability distribution of scattering angles after every scattering event were calculated according to Mie theory with the cell size and the refractive index inside and outside of the cells, with a 99% chance the scattering angle will fall between +/−6 degrees. We then counted the number of photons which escape from the air-tissue surface in the backward direction and plotted out the steady state distribution of the backscattered photons over the radial distance from the emission point.

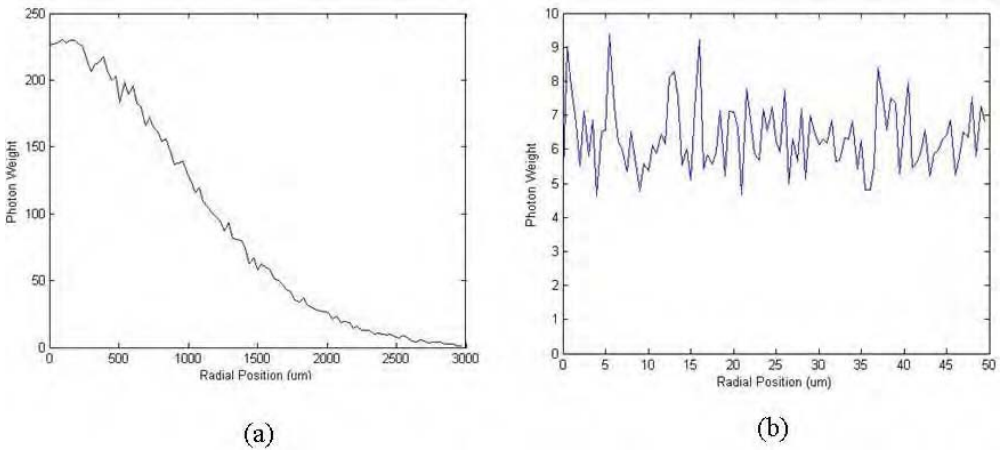

Fig. 3. Monte Carlo simulation of forward propagating and subsequently backscattered SHG photons which reach the object plane.(a) Steady state radial distribution of the backscattered SHG photons over a large range of radial position (3mm) (b) The same distribution over a short radial range (50um)

The simulation results are shown in Fig. 3. Figure 3(a) shows the steady state distribution of the forward propagating and subsequently backscattered SHG photons which reach the object plane, over a large range of radial positions i.e. from the center to 3mm away from the

#124594 - $15.00 USD Received 23 Feb 2010; revised 16 Apr 2010; accepted 19 Apr 2010; published 5 May 2010

emission point. Figure 3(b) shows the same distribution over a short range i.e. from the center to only 50um away from the emission point, which is the length scale of our largest pinhole setting (where the pinhole-bearing foil has been punched out). We can see from Fig. 3(a) that over a large length scale the forward propagating and subsequently back-scattered SHG photon intensity decays exponentially with the distance from emission point, which agrees with previous literature [11]. But from Fig. 3(b) we can see over a very short range of 50 um, the range covered by our pinhole settings and where the diffusion approximation does not hold [11], the intensity of forward propagating and subsequently back scattered SHG photons is constant and does not depend on distance from the focal volume.

2.3 Fitting model

To measure collagen fiber SHG F/B ratio in vivo with only the epi-detection objective, we will generate a series of collagen fiber SHG images, in the backward channel, through a series of confocal pinholes of different sizes which correspond to a diameter in the object plane ranging from 0.874 um to 102 um (see 3.1 below). As discussed above, the SHG signal we collect after the pinhole is a mixture of both the direct backward propagating SHG and the forward propagating and subsequently backscattered SHG. To analyze our experimental data we model the image in the pinhole plane of the direct backward propagating SHG signal plane as a Gaussian spot [12], while the forward propagating SHG that subsequently backscatters is modeled as a uniform distribution over these length scales (based upon the results of our Monte Carlo simulation, as described above). So the total SHG signal intensity distribution on the object plane can be expressed as:

$$I_{SHG}(r) = B\exp[-2(\frac{r}{\omega})^2] + FC, \tag{1}$$

where ω is the e−2 Gaussian spot size of the direct backward propagating SHG, F and B are absolute intensities of forward and backward propagating SHG signals, the parameter C relates the initial forward propagating signal intensity to the average intensity of the uniform distribution of SHG light that reaches the object plane, and is a function of scattering and absorption properties of the underlying tissue. Alternatively, this expression can be written in another way,

$$I_{SHG}(r) = B[\exp[-2(\frac{r}{\omega})^2] + \frac{F}{B}C], \tag{2}$$

where F/B represents the collagen fiber SHG F/B ratio.

When we generate collagen fiber SHG images through a series of confocal pinholes of different sizes, each pixel on that image represents an integration of the total SHG signal over the pinhole area

$$I_{pixel} \propto \int_0^{2\pi} d\theta \int_0^R \left\{ \exp[-2(\frac{r}{\omega})^2] + \left(\frac{F}{B}\right)C \right\} r dr, \tag{3}$$

where R is the size of the pinhole with respect to Gaussian spot size of the direct backward propagating SHG, i.e. R = rpinhole/ω. If the pixel intensities at various pinhole sizes are normalized to the maximum pixel intensity at the largest pinhole size, the relative pixel intensity is a function of relative pinhole size R:

$$I_{rel}(R) = \frac{\int_0^{2\pi} d\theta \int_0^R \left\{ \exp[-2(\frac{r}{\omega})^2] + \left(\frac{F}{B}\right)C \right\} r dr}{\int_0^{2\pi} d\theta \int_0^{R_{\max}} \left\{ \exp[-2(\frac{r}{\omega})^2] + \left(\frac{F}{B}\right)C \right\} r dr}, \tag{4}$$

#124594 - $15.00 USD Received 23 Feb 2010; revised 16 Apr 2010; accepted 19 Apr 2010; published 5 May 2010

where Rmax is the largest pinhole size in our system. With this expression we can plot the relative pixel intensity versus pinhole size and fit the data to produce (F/B)C. In order to determine F/B we must then eliminate C, the fraction of signal which originally propagates in the forward direction but is eventually backscattered by the tissue and reaches the pinhole plane. This can be done by introducing into the sample a reference of known F/B ratio, whose C value is the same. In these experiments we used blue fluorescent polystyrene beads (peak λem = 424nm) sprinkled onto the sample surface. The quantity (F/B)C is then determined for both the calibration beads in the image, as well as the fibers of interest. Next, the correction factor that is required to convert the measured values of bead (F/B)C to the known value of F/B is determined, and the previously unknown value of fiber F/B is determined from the measured (F/B)C using the same correction factor:

$$\frac{\textit{measured collagen SHG F / B Ratio}}{\textit{measured beads TPEF F / B Ratio}} = \frac{\textit{real collagen SHG F / B Ratio}}{\textit{real beads TPEF F / B Ratio}}. \quad (5)$$

To illustrate the fitting function given by Eq. (4) in the case of the typical backscattering fraction C = 0.001 and Rmax = 28 we can plot out the relative pixel intensity v.s. pinhole size curves at various collagen fiber SHG F/B ratios in Fig. 4:

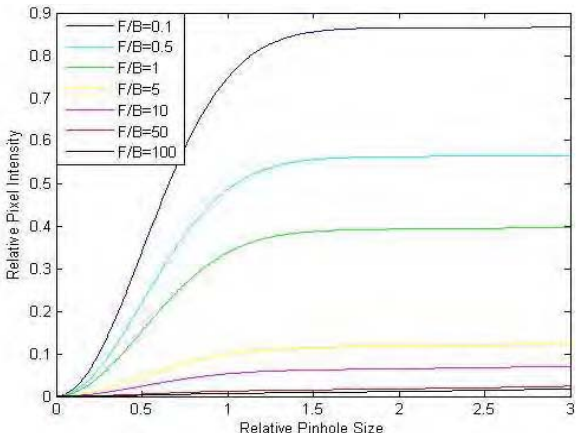

Fig. 4. Relative SHG intensity vs. relative pinhole size curves at different collagen SHG F/B ratios, based upon Eq. (4). The relative SHG intensities equal 1 at a pinhole size of r = Rmax = 28.

From this plot one can see the sharp curvature due to the Gaussian distribution of direct back-propagating SHG (most evident in the steep early rise of the curves with small values of F/B) and the slow and steady rise due to forward-propagating light that is subsequently backscattered and produces a diffuse signal which does not vary with r (most evident in the slow rise of the curves with large values of F/B). This reveals the utility in punching out one of the metal foils containing a pinhole from the pinhole turret of the scanner, as this produces one pinhole of extremely large size (R = 28 in the case of the Fluoview 300) whose radius is far from the initial sharp curvature due to the Gaussian distribution of direct back-propagating SHG, allowing the collection of a great deal of the diffuse forward-propagated signal.

3. Results

3.1 Determining backward propagating SHG spot size on the pinhole plane

In order to produce the required plot of SHG signal versus pinhole size and fit it with our model, we must first determine the sizes of the pinholes, relative to the Gaussian spot size of the direct backward propagating SHG on the pinhole plane. Since we are determining the spot size in the pinhole plane of the direct backward propagating SHG, we must avoid significant backscattering of the forward propagating SHG. Therefore rat tail collagen samples were fresh frozen and sectioned into 10um thin slices, spread out on a cover slip and dried

#124594 - $15.00 USD Received 23 Feb 2010; revised 16 Apr 2010; accepted 19 Apr 2010; published 5 May 2010

overnight in a refrigerator for good adhesion between sample sections and cover slip. The cover slip was then flipped over with the sample side facing down, submerged in PBS and the excitation beam transmitted through the cover slip. The sample was submerged in saline to minimize the refractive index change and thus reduce the subsequent backscattering of the forward propagating SHG. The saline container is a cup with 4 cm diameter and 4 cm depth. It was painted black to absorb forward propagating SHG that goes through the sample section (see Fig. 5).

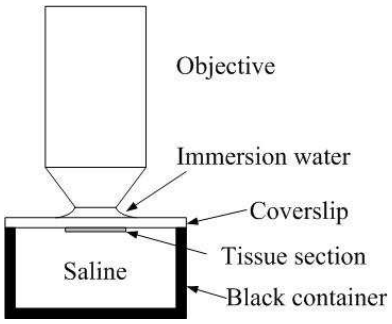

Fig. 5. Configuration of objective, sample and scatterer holder

To determine the size of the image of the SHG spot in the pinhole plane, we measured the SHG spot directly with a CCD camera (SPOT RT3, SciTech) at the intermediate image plane depicted on Fig. 1. The SHG spot in the pinhole plane is just a magnified version of the spot we captured with the CCD camera with a magnification factor of the ratio of the focal length of the pupil lens and collection lens.

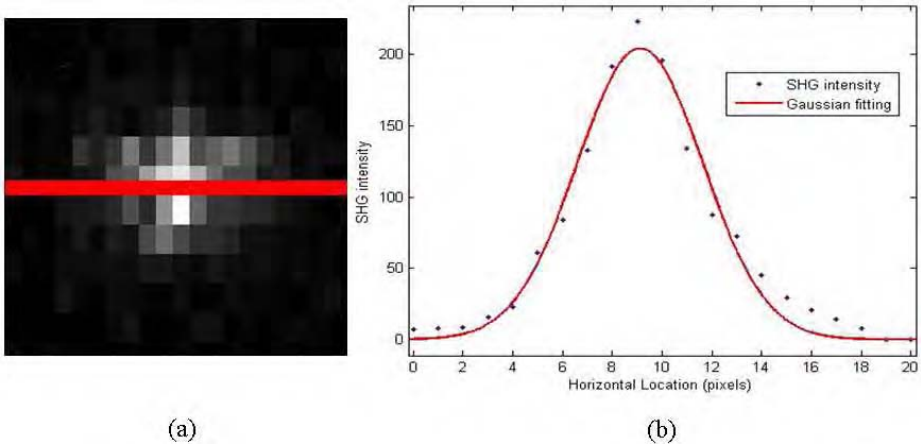

Fig. 6. Determination of SHG spot size. (a) CCD captured image of SHG focal spot after the tube lens (b) SHG intensity along the straight line that goes through the center of SHG spot. The red straight line in (a) is the line along which SHG intensities are measured. The red curve in (b) is the Gaussian fit to the intensities we measured in (a)

As shown in Fig. 6(a) above, we drew a straight line through the center of the SHG spot captured by CCD camera, and measured SHG intensity along this line. The SHG intensity vs. horizontal location data set was then plotted in Fig. 6(b) as a series of separate points, and fitted to a Gaussian model producing an average spot size in the intermediate image plane of 9.34 pixels or 69 um. Taking into account the magnification factor of the pupil and collector lens, the average pinhole plane spot size of the backward propagating SHG is therefore 236.8 um. We already knew the absolute diameters of the five pinholes on the pinhole turret are 60um 100um 150um 200um to 7000um respectively (7000um corresponds to the location in the pinhole turret where we punched out the pinhole-bearing metal foil). That corresponds to

#124594 - $15.00 USD Received 23 Feb 2010; revised 16 Apr 2010; accepted 19 Apr 2010; published 5 May 2010

0.24 ω, 0.4 ω, 0.6 ω, 0.8 ω and 28 ω, where ω stands for the e−2 SHG spot size in the pinhole plane.

3.2 Measurement of SHG intensity varied with pinhole size

To evaluate our new method we chose the rat tail tendon, a sample whose SHG properties have been well studied [1]. A whole rat tail was removed from a previously sacrificed animal (removal from the animal is not necessary for the technique but is convenient for handling the sample). To generate a clear SHG image of the tendon in particular (to match the sample previously studied in the literature) we peeled a thin layer of outer skin off the rat tail at the location of interest and exposed the tendon beneath it. We then put the rat tail on a glass slide, with the exposed collagen fiber facing up and we put another coverslip on top of the collagen fibers to ensure a stable sample. The rat tail and coverslip were then fixed on the glass slide with plastic tape and the collagen fibers were imaged though the coverslip. Note that, unlike previous methods which measure F/B with a second detector for the forward-propagating SHG, the tendons remained within the ~1cm diameter tail.

We prepared whole rat tail samples from 5 separate animals (see Fig. 7). On each rat tail we chose 5 image fields. And for each image field we took 5 back detected SHG images with the pinhole size varied from 60um 100um 150um 200um to 7000um, plus one image with no sample in order to quantify the background noise. One of these image sets is shown below.

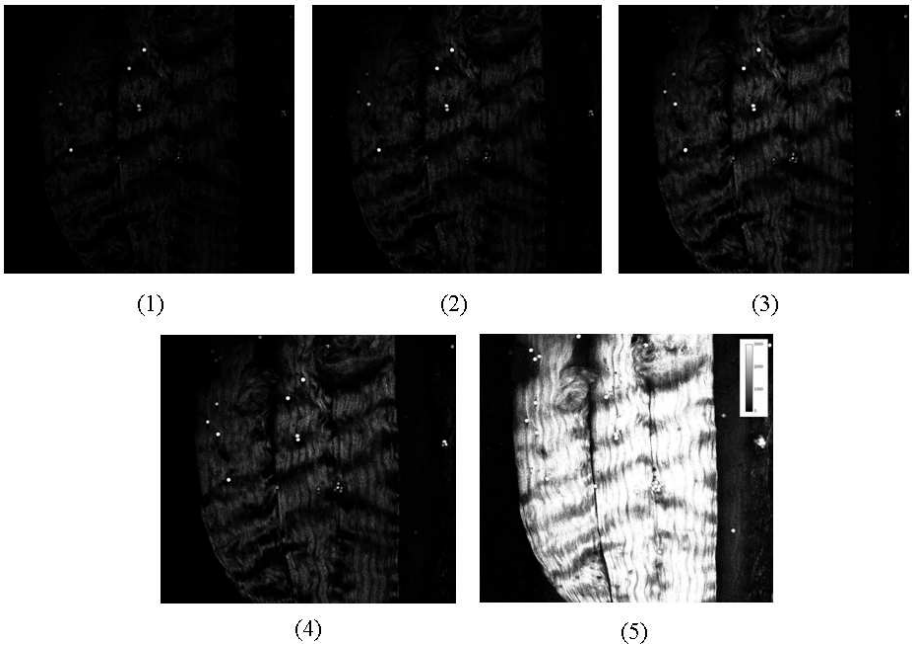

Fig. 7. In vivo SHG images of rat tail collagen fibers in an intact rat tail. Images 1-5 are SHG images of the same ROI when the size of the pinhole varied from 60um, 100um, 150um, 200um, to 7000um, respectively. The bright spots are blue fluorescent polystyrene beads for calibration. Images are 600 um across.

3.3 Curve fitting and prediction of collagen SHG F/B ratio

In each set of images, we picked 5 small regions of interest (ROIs) around collagen fibers and 3 regions of interest around the calibration beads. ROIs were drawn around fibers that extended over at least ~100 um in the image plane, to ensure that fibers were close to perpendicular to the optical axis. A length 100 um in an optical section of ~12 um thickness (e−2 z diameter of the PSF) corresponds to a maximum angle in the object plane of ~7 degrees. Signal intensities in these collagen and beads ROIs were measured with ImageJ,

#124594 - $15.00 USD Received 23 Feb 2010; revised 16 Apr 2010; accepted 19 Apr 2010; published 5 May 2010

background was subtracted, and signal intensities were normalized so that the maximum intensity measured with the largest pinhole was set to 1. The average relative SHG intensity of all 25 collagen ROIs (5 ROIs in each of 5 image stacks) and average relative TPEF intensity of all 15 beads ROIs in one rat tail vs. relative pinhole size plot is shown below. Note the separation between the collagen fiber curve and the bead curve due to the different F/B ratios of rat tail collagen and fluorescent calibration beads.

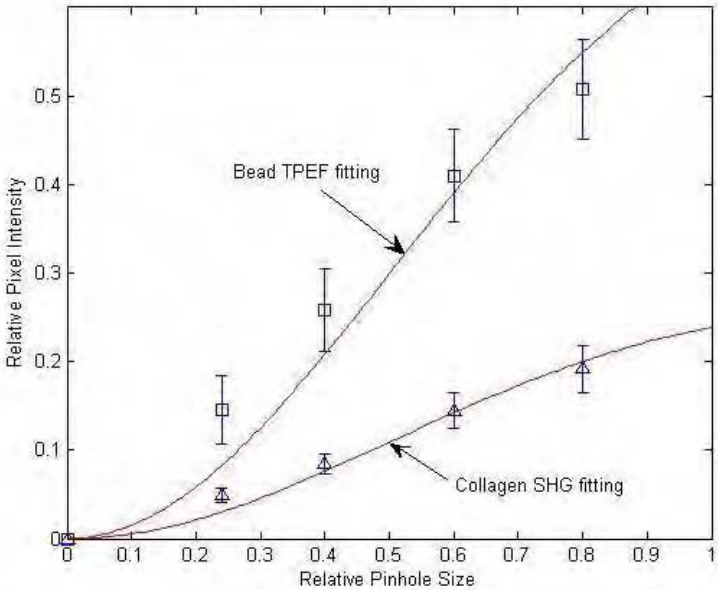

Fig. 8. Epidetected total collagen SHG intensity (blue triangles), or total bead TPEF intensity (blue squares) vs. pinhole size, fit to the model given by Eq. (4) (red lines). The horizontal axis is pinhole size in units of backward propagating SHG spot size on the pinhole plane i.e. fraction of ω. The vertical axis is normalized SHG intensity. Note that the fitting curves identically equal 1 when the pinhole size reaches R = 28, whose data point is not shown, and that the intensity information for R = 28 provides the normalization value and hence is included in the overall fit.

As described above, for one rat tail we measured relative intensity in 25 collagen ROIs and 15 bead ROIs. For each ROI 5 relative intensities were measured with size of the pinhole varying from the smallest to the largest. Average relative SHG intensity of all 25 collagen ROIs and average relative TPEF intensity of all 15 bead ROIs, as shown in Fig. 8, were considered a set of data for one rat tail. We then fit this set of real measured data to the model given in Eq. (4) and calculated the rat tail collagen fiber SHG F/B ratio in one animal by eliminating C using Eq. (5). This data collection/averaging/curve fitting/calculation process was repeated 5 times to calculate rat tail collagen fiber SHG F/B ratio in 5 animals. The results are listed in Table 1 below.

Table 1. Results of in vivo measured rat tail collagen SHG F/B ratio

	Animal I	Animal II	Animal III	Animal IV	Animal V	Average
F/B ratio	2.10 ± 0.19	1.81 ± 0.30	2.50 ± 0.34	1.34 ± 0.13	2.26 ± 0.23	2.00 ± 0.45

For each animal, means ± 95% confidence intervals are presented, with the data from 25 ROIs being pooled to produce a single curve fit for each animal. The average value for the 5 animals is then presented ± the standard deviation.

To verify the validity of our method using thick samples and only epi-detection, we also directly measured rat tail collagen SHG F/B ratio with both forward and backward detectors and with the sample sectioned in ~10um thin slices, as previously described [4]. In summary,

#124594 - $15.00 USD Received 23 Feb 2010; revised 16 Apr 2010; accepted 19 Apr 2010; published 5 May 2010

the SHG image captured in the forward detector was divided by the SHG image captured in the backward detector. We then averaged SHG F/B ratio over all pixels within collagen fibers and ignored all pixels outside the collagen fibers. The scattering of the tissue, though very low in this case, was corrected for by measuring the F/B ratio of the TPEF signals from 10um diameter calibration fluorescent beads.

The measurement results from 5 animals, using forward and backwards detectors, are listed in Table 2.

Table 2. Results of in vitro measured rat tail collagen SHG F/B ratio

	Animal VI	Animal VII	Animal VIII	Animal IX	Animal X	Average
F/B ratio	1.43 ± 0.80	1.22 ± 0.27	2.29 ± 0.49	1.75 ± 0.50	2.11 ± 0.86	1.76 ± 0.45

For each animal, means ± standard deviations are presented from 5 F/B measurements. The average value for the 5 animals is then presented ± the standard deviation.

The overall average F/B ratio from 5 animals is 1.76+/–0.45. This result was not statistically significantly different from our measurement using only the epi-detection objective lens and the model given by Eq. (4) (Student's t-test $p = 0.42$) demonstrating that the results from the two methods are in good agreement. To evaluate the new method at a higher NA we also measured the F/B ratio using a 0.8 NA lens, producing a value for F/B (1.37+/–0.28) which is again not statistically significantly different from the direct measurement using forward and backwards detectors ($p = 0.17$ $N = 5$).

4. Discussion

In this paper, we present a method to measure the SHG F/B ratio with only an epi-detection objective lens, allowing measurement on thick tissue samples. In our demonstration we used the whole rat tail (~1 cm thick), with the rat removed for convenience, but the technique is equally applicable to a live specimen. By obviating the need for thin sectioning of the sample, this technique provides the opportunity to do time-dependent studies, as well as the possibility of use in an endoscopic setting. This is significant because SHG F/B ratios have been shown to be of interest in discriminating skin with Osteogenesis Imperfecta [2] from normal dermis [2] and SHG F/B ratio measurements have been used to help determine the organization of fibrillar collagen in samples such as breast tumor models [4], in rat tail tendon [1], cellulose [3], mouse Achilles tendon [8], muscle fascia [8], and ovarian cancer [7] (although see 4.2 Limitations, below). Furthermore, the confocal pinholes used in this technique are available in most commercial two photon microscopes, allowing the measurement of the SHG F/B ratio in intact specimens without addition of new equipment (assuming one is already using a two-photon microscope to study SHG) or extensive equipment modification (except for a single dichroic and filter inserted in the dichroic holder of the scanbox, and the punching out of one of the pinhole settings to produce one very large pinhole).

4.1 Sensitivity

In order to determine the radial intensity distribution of the forward propagating and subsequently backscattered SHG using a Monte Carlo simulation, the tissue scattering parameters we used in the simulation were $\mu a = 0.7$ cm–1 and $\mu s = 150$ cm–1, which are typical values for 405 nm light [10]. However, the scattering properties of tissue vary over a large range among different organs throughout the body, and it is reasonable to wonder if this fitting model is good for all types of tissues from different organs. To determine this we varied the scattering parameters over a large range and repeated the Monte Carlo simulation with the results shown in Fig. 9 and Fig. 10.

#124594 - $15.00 USD Received 23 Feb 2010; revised 16 Apr 2010; accepted 19 Apr 2010; published 5 May 2010

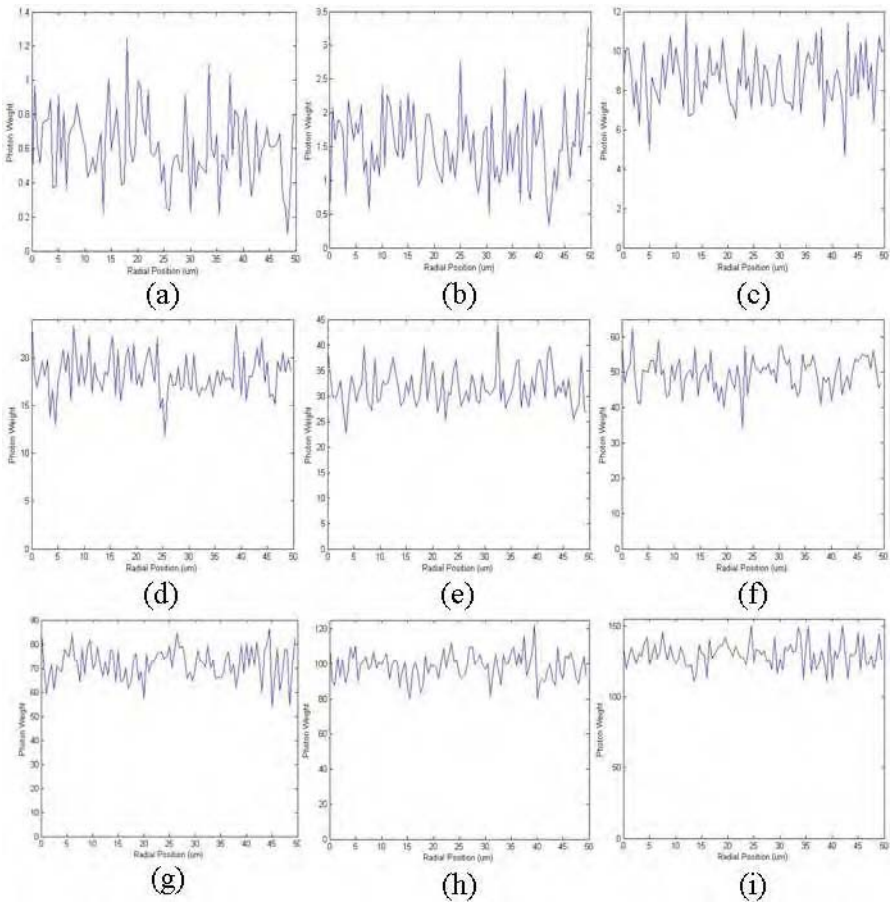

Fig. 9. Monte Carlo simulation of forward propagating SHG that is subsequently backscattered and reaches the object plane, with varying μs. Steady state radial distribution of the backscattered SHG photons when (a) μs = 100 cm–1 (b) μs = 150 cm–1 (c) μs = 200 cm–1 (d) μs = 250 cm–1 (e) μs = 300 cm–1 (f) μs = 350 cm–1 (g) μs = 400 cm–1 (h) μs = 450 cm–1 (i) μs = 500 cm–1. In each case μa = 0.7 cm–1

#124594 - $15.00 USD Received 23 Feb 2010; revised 16 Apr 2010; accepted 19 Apr 2010; published 5 May 2010

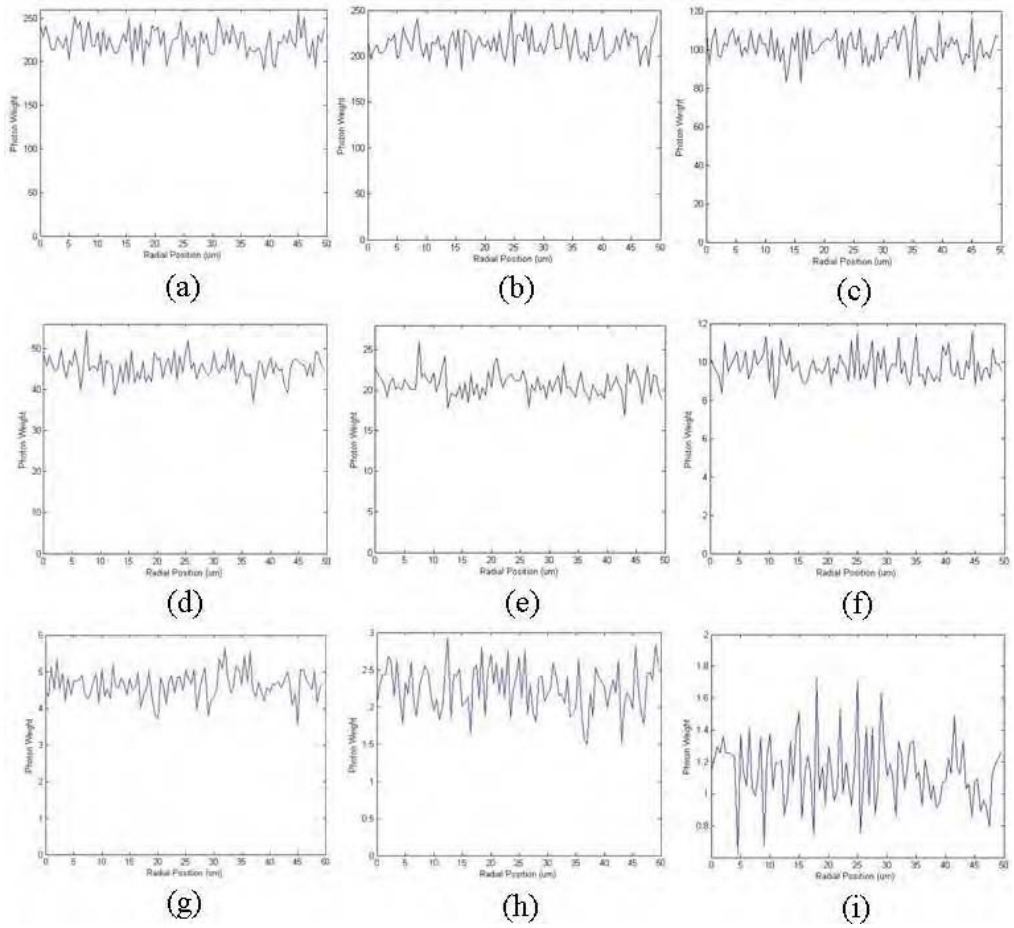

Fig. 10. Monte Carlo simulation of forward propagating SHG that is subsequently backscattered and reaches the object plane, with varying μa. (a) Steady state radial distribution of the backscattered SHG photons when (a) μa = 0.05 cm–1 (b) μa = 0.1 cm–1 (c) μa = 1 cm–1 (d) μa = 2 cm–1 (e) μa = 3 cm–1 (f) μa = 4 cm–1 (g) μa = 5 cm–1 (h) μa = 6 cm–1 (i) μa = 7 cm–1. In all three cases μs = 500 cm–1

We can see from the simulation results that when μa decreases or μs increases more forward propagating SHG photons reach the object plane after subsequent backscattering; and when μa increases or μs decreases less reach the object plane. However, over a range of scattering parameters in our Monte Carlo simulations that are comparable to values found at these wavelengths in the literature [10], varying μa and μs does not alter the distribution of light exiting the tissue over the 0-50 um length scale, and it remains a constant, independent of radial position (a slope of zero is within the 95% confidence interval). We therefore conclude that within this small region of the object plane close to the optical axis, which is the region covered by our pinhole distribution, the radial intensity distribution of the backscattered SHG is not affected by a wide variety of tissue scattering parameters, and this fitting model is therefore applicable for tissue from diverse organs.

4.2 Limitations

This technique has two significant limitations. As shown in Fig. 4, when the F/B ratio increases, the separation between two SHG intensity vs. pinhole size curves decreases. Using a reasonable value for C [8], Fig. 4 shows that when the collagen fiber SHG F/B ratio is significantly more than ~5, the two curves are so close that they are not likely to be

#124594 - $15.00 USD Received 23 Feb 2010; revised 16 Apr 2010; accepted 19 Apr 2010; published 5 May 2010

distinguishable assuming typical variation in experimental data (such as shown in Fig. 8). This implies that the new method might not be applicable for samples with collagen fiber SHG F/B ratios significantly higher than ~5. To illustrate this, we applied this method to measure the SHG F/B ratio of collagen fibers in intact mouse skeletal muscle fascia (with overlying skin removed to allow access). Using the new technique, we produced a value of the collagen fiber F/B ratio in vivo of 5.05+/–0.81 (N = 5) while after extracting the fascia, mounting it between two coverslips and directly measuring SHG F/B ratio with two objective lenses we produced a value of 5.56+/1.03 (N = 5), which was not statistically significantly different (p = 0.43). We also applied this method to measure the SHG F/B ratio of collagen fibers in 4T1 breast tumor models. According to our previous work the true collagen fiber SHG F/B ratio in 4T1 mouse breast tumor is ~30. We measured collagen fiber SHG F/B ratio in vivo in whole tumor samples from 5 different animals (25 ROIs per animal), and the result is 6.64+/–2.98 (data not shown). As predicted, as the F/B becomes significantly larger than ~5, the result becomes inaccurate and noisy, with a greater relative standard deviation, because of the normal random noise in the experimental data combined with the insensitivity of this new technique to large F/B values. Fortunately, our data and published studies reveal that the F/B ratio in many biological samples is at or below five, including in the rat tail tendon (F/B~1), skeletal muscle fascia (F/B~5), cellulose (F/B~4), ovarian cancer (F/B ~3.4), and dermis with (F/B~3.4) and without (F/B~2.64) Osteogenesis Imperfecta [1–3,7,8]. Care must be taken when this technique produces F/B ratios significantly greater than five.

The second limitation arises from the fact that this technique assumes there is no subsequent scattering of back-propagating SHG signal. Hence it is limited to the surface, or extremely shallow imaging depths, of the sample and is suitable for quantifying F/B ratios on intact thick tissue samples, but not in intact thick tissue samples.

5. Conclusion

In this paper, we present a method to measure SHG F/B ratio suitable for intact tissue samples without sectioning, using just the epidetection objective lens. The method requires minor modification of the dichroics, filters, and confocal pinholes used in most commercial two photon microscopes and hence minimizes the purchase of new equipment. This allows F/B ratio measurements to be done in a dynamic fashion, and offers the possibility of endoscopic measurements. This technique is sensitive to F/B values up to ~5 and within this range are a variety of interesting and clinically relevant materials, tissues, and disease states, including tendon, fascia, cellulose, ovarian cancer, and dermis with and without Osteogenesis Imperfecta. The fact that OIM is within the range of this technique's sensitivity offers the attractive possibility of a non-invasive optical diagnosis of that disease, using a single objective lens, without biopsy samples being removed from the patient.

Acknowledgements

We thank Dr. Jerome Mertz for helpful conversations. This work is supported by a Department of Defense BCRP Pre-doctoral Traineeship Award (W81XWH-08-1-0323) to Xiaoxing Han, a Department of Defense BCRP Era of Hope Scholar Award (W81XWH05-1-0396), and a Pew Scholar in the Biomedical Sciences Award to Edward Brown III.

#124594 - $15.00 USD Received 23 Feb 2010; revised 16 Apr 2010; accepted 19 Apr 2010; published 5 May 2010